第 41 卷 第 4 期：1154-1166 高电压技术 Vol.41, No.4: 1154-1166
2015 年 4 月 30 日 High Voltage Engineering April 30, 2015
DOI: 10.13336/j.1003-6520.hve.2015.04.013

Trapping Parameters and Their Relation to Insulation Status of XLPE Cables

Ning Liu[1], George Chen[1,2], Yang Xu[2]
(1. University of Southampton, Southampton, SO17 1BJ, UK; 2. Xi'an Jiaotong University, Xi'an 710049, China)

Abstract: Space charge issues have raised many attentions in recent years, especially in high voltage direct current (HVDC) application. Space charge accumulation in insulation system will give rise to acceleration of ageing and even cause premature failure of the material. However, from another angle, space charge might be also considered as a diagnostic tool of ageing for insulation materials. In this paper, a trapping-detrapping model has been developed to estimate trapping parameters of cross-linked polyethylene (XLPE) cable sections, which were taken from different HVAC operation conditions of 12 years and 8 years. The results reveal that, for both cable sections, samples from the inner location have the greatest trap density and the deepest trap depth. Additionally, breakdown strength tests and FTIR (Fourier-transform infrared) measurements on those samples have been carried out. From FTIR measurement results, the degree of oxidation among three layers could be found by the carbonyl index values. The oxidation degree of aged cable at the outer layer is higher than that at the other two layers probably because of the most sufficient contact with oxygen. Also, it has been noticed that the results from these measurements show some correlations with the estimated trapping parameters, especially for breakdown strength.

Key words: charge injection; charge trapping/detrapping; trap density; XLPE insulation; ageing; breakdown strength

0 Introduction

Space charge accumulation in insulation materials received significant attention in recent two decades as the presence of space charge led to local electric field distortion and may shorten insulation lifetime by accelerating degradation and ageing in materials. From the models established in reference [1-3], it has been pointed out that space charges are both cause and effect of ageing and these models showed how space charges quantitatively influence on insulation lifetime.

Due to the wide band gap of insulation materials, electrons might reside within the band gap without jumping to conduction band directly. And those localized states, or namely 'traps', with density N, offer charge carriers an intermediate state at certain energy level, which is defined as the 'trap depth', E_t. Also, the ability of these traps to capture charge carriers relates to the trapping cross-section area S. Here, under the assumption of Coulombic attractive trap[4], and one trap could only accommodate one charge carrier, we take the cross-section area as $S=\pi r^2$, where r is distance between the trap and its charge carrier.

Above all, trap density N, trap depth E_t, and trapping cross-section area S are generally called trapping parameters. They depict the attributes of traps. Many investigators have put efforts on estimation of the trapping parameter of insulation materials in the recent decade. In reference [5], Chen proposed a trapping-detrapping model based on two energy levels and, thereafter in references [6] and [7], by applying the model in reference [5], trapping parameters of low-density polyethylene (LDPE) and gamma-irradiated LDPE were estimated through the pulsed electro-acoustic depolarization (PEA) method. The comparison between results of these two materials indicated that the physical and chemical changes brought by the irradiation process alter the trapping parameters, especially for trap density and deep trap depth. Moreover, Dissado *et al*. have proposed another trapping-detrapping model to evaluate trapping parameters of different time-aged XLPE cable peelings[8-9]. The basic ideas of these two approaches are quite sim-

ilar: 1. Both numerical models are applied to condition of charge relaxation after the removal of an external voltage; 2. The trapping parameters are obtained by fitting curves of specific model parameters with experimental data from depolarization tests; 3. Observed charge dynamics during volts-off condition was considered as the decay of trapped charges, *i.e.* mobile charges generated the detrapping process were assumed escaping from the sample instantly, and only detrapping process was taken into consideration. Here, in the present paper, a new model is proposed, based on first two ideas of previous models but improving on those models by considering charge re-trapping processes. This refers to possibility that detrapped charges might get captured by vacant traps before they outflow from the local charge region. Moreover, an innovative feature inspired from the model in reference [5] is to treat traps with a range of energy levels as traps at two equivalent levels: shallow traps and deep traps. These two types of traps probably relate to physical (shallow) and chemical defects (deep) respectively[10]. Therefore, in the present paper, the idea was adopted during modeling.

Samples used in this work are XLPE films peeled from cable sections operated for 12 years and 8 years. Films were grouped as outer, middle and inner layers, in accordance with their radial locations on cable sections to investigate differences in trapping parameters for samples from different depths.

Apart from the estimation on trapping parameters, in the present research, an attempt has been made to reflect changes in trapping parameters with one of the important dielectric properties, *i.e.* DC breakdown strength of materials. Firstly, DC breakdown measurements have been tested on the same type of samples as those used for the PEA measurements. It has been found that the breakdown strength can be related to the estimated trap density and depth of XLPE material. In addition, FTIR measurements were made on those XLPE specimens from the same areas to understand thermal oxidation hence carbonyl index was calculated. The results cannot demonstrate a clear relationship between the oxidation degree and trapping parameters but it was found that carbonyl index of XLPE peelings depends on the radial locations in the cable insulation.

1 Model of Charge Dynamics

Poole-Frenkel effect occurs in the material with wide band-gap (*e.g.* insulating material or insulator) where electrons/holes can reside. Theeffect demonstrated in the Pool-Frenkel mechanism that the potential barrier height of Coulombic attractive traps is deducted by Coulombic force between these charge trapping centres and charge carriers. By considering the effect of poling electric field in Equation (1), the trap depth E_t could be reduced in the field direction by value ΔV_F, *i.e.*

$$E_t' = E_t - \Delta V_F(E) \tag{1}$$

where the maximum reduced height $\Delta V_F(E)$ of the barrier in the field direction is

$$\Delta V_F(E) = 2\left(\frac{q^3 E}{4\pi\varepsilon_0\varepsilon_r}\right)^{1/2} \tag{2}$$

and E is the applied field; q is unit charge amount; ε_0 is vacuum permittivity; and ε_r is the relative permittivity of the target material. This maximum reduced height happens when the Coulombic force between electrons/holes and ionised donors/acceptors (*i.e.* traps) are equal to the electrostatic force under the applied field (further details in reference [11]). Thus, the rate of thermal excitation of trapped electrons/holes from localized states to the conduction/valence band could be given by

$$R_{esc} = n_t v_0 \exp\left(-\frac{E_t'}{kT}\right) \tag{3}$$

where n_t is the trapped charge density; T is temperature (300 K used in the present paper); k is the Boltzmann constant(about 1.38×10^{-23} kg·m^2·s^{-2}·K^{-1}; and v_0 is the attempt to escape frequency (about 2×10^{13} Hz at room temperature[7]). It is worth mentioning here that the model is applied under the condition when the applied electric field is removed.

Moreover, the rate of capture by trap sites R_{cap} should be proportional to the number density of free charges which have been released into the conduction/valence band n_f and the number of unoccupied

trap site density($N-n_t$), given N is total trap density

$$R_{cap} = n_f (N - n) v_{th} S \quad (4)$$

where v_{th} is the thermal velocity (=3.7×10^5 m/s for holes in polyethylene material[7]) of electrons or holes and S is capture cross section area of trap sites for charge carriers.

In references [6-9], these models consider observed chargesas trapped charges. The free charge carriers, or said mobile charges will flow away from local space charge region via extraction from adjacent electrode or flowing into the other side of electrode dependent upon the direction of Coulombic force they experienced. However, in the models applied in references [6-9], those mobile charges were thought to be flowing instantaneously from their original locations. Here in the present model, we take consideration of transit time Δt or detrapped charges' out flowing from the local charge region without retrapping is taken into consideration. And we made an important assumption that during Δt, the charges might be re-captured by unoccupied traps and the free charge carrier density generated by excited charges could be expressed as: $n_f = \int_t^{t+\Delta t} R_{esc} \mathrm{d}t$. For the estimation of Δt, we use: $\Delta t = \frac{D}{v_d}$ Here, D is the averaged distance from original location to the boundary of space charge region. Typically, in our measurements, the positive charge peak is dominant. Since the width of positive space charge region is around 80 μm (see typical PEA results in Section 4). Since holes move boundaries of charge region inboth directions dependent on the force, D is approximated as half of the half positive peak width, *i.e.* 20 μm. And under electric field of the order 10^6 V/m, which is the approximated electric field after the removal of the external voltage in the volts-off measurements, the drift velocity is at an order of 10^5 m/s[12]. As a result, the transit time Δt could be approximated as $\Delta t = \frac{D}{v_d} = 2\times10^{-10}$ s. As this time is too short for charge escaping rate to be substantially changed, the free charge carrier density could be estimated as $n_f = R_{esc}\Delta t$. And changing rate of trapped charge density n_t is

$$\frac{\mathrm{d}n_t}{\mathrm{d}t} = R_{cap} - R_{esc} = n_t v_0 (\Delta t (N - n_t) v_{th} S - 1) \exp(-\frac{E_t'}{kT}) \quad (5)$$

Solving Equation (5), we could have a solution in the form of

$$n_t = a \coth(bt + c) - a \quad (6)$$

where a and b are:

$$a = \frac{1 - \Delta t (N - n_t) v_{th} S}{2\Delta t v_{th} S} \quad (7)$$

$$b = v_0 \exp(-\frac{E_t'}{kT}) \frac{1 - \Delta t (N - n_t) v_{th} S}{2} \quad (8)$$

Parameter c will be decided at the initial condition, where trapped charge density n_0 at t=0, we have

$$n_0 = n_t(0) = a \coth(c) - a \quad (9)$$

When we extend the model described by Equation (5) to two equivalent level traps, *i.e.* shallow and deep traps

$$n_t = a \coth(bt + c) - a + d \coth(et + f) - d \quad (10)$$

where a, b and c are parameters for shallow traps, and d, e and f are for deep traps, comparable to a, b and c respectively.

Furthermore, there is evidence that deeper traps in dielectrics should have a smaller cross-section area[13]. Physically, it can be explained that smaller capture radius will give rise to a greater Coulombic attractive force upon on charge carrier, hence forming a deeper trap from which it is harder for charge carrier to escape. Especially in reference [14], it was proposed that he binding energy W of a Coulombic trap to charge carrier is inversely proportional to radius of the trap r. The binding energy W directly determines the trap depth E_t. The larger W becomes, the tighter the charge carrier is bound to the trap, *i.e.* trap depth should be deeper. Here, it is assumed that E_t is proportional to W and, since trapping cross-sectional area $S=\pi r^2$, S is inversely proportional to E_t^2.

According to previous works [6], [7] and [15], the estimated value for cross section area ranges from 10^{-16} to 10^{-18} m^{-2}.

In reference [16], it was proposed that cross section area should be field-dependent: experimental data in reference [16] (see Fig.1) shows that the trapping cross section area for Coulombic attractive traps is proportional to E^{-15} below the threshold field E_{th} and

proportional to E^{-3} above E_{th}.

Anaveraged field of E_a across the positive charge region could be approximated by using the mean trapped charge density in the region, n_t. Hence, from the Gauss's law, we have[17]

$$E_a = \frac{n_t q l}{2\varepsilon_0 \varepsilon_r} \tag{11}$$

where l is the width of the positive charge layer, ε_0 is vacuum permittivity, and ε_r is the relative permittivity of polyethylene. Since the trapped charge density n_t is a function of time, E_a should be dependent on both time and cross section area S. However, for the sake of simplicity, n_t for each type of samples is approximated as a mean value $\overline{n}_t$ by averaging values of n_t following mean value theorem of integral over time-span of the depolarization measurement, *i.e.*

$$\overline{n}_t = \frac{\int_{t_0}^{t_e} n_t(t)\mathrm{d}t}{t_e - t_0} = \frac{\int_{t_0}^{t_e} (a\coth(bt+c) - a + d\coth(et+f) - d)\mathrm{d}t}{t_e - t_0} \tag{12}$$

where t_0=0 s and t_e=1 800 s, and t_e is the end time of all depolarization tests. Applying Equation (12) to measurement data from depolarization test of two cable peelings from three different layers (see details in next section), the averaged trapped charge density $\overline{n}_t$ for each sample can be obtained. Based on positive charge layer thickness l is 80 μs, and ε_r=2.3 for polyethylene, aroughly approximated value for E_a could be obtained as in Table 1.

From references [6-7], when E_{t1}=1 eV, the trapping cross-section area is around 6.60×10^{-17} m^{-2} and the trapped charge density in depolarization measurement is around 1.00×10^{-8} C. By using the charge layer thickness and electrode area in references [6-7], numerical charge density was calculated as 1.97×10^{19} m^{-3}. Therefore, the electric field after the removal of the applied voltage in references [6-7] is estimated as 3.87 MV/m. In light of the *E*-*S* relationship in Fig.1, the trapping cross-section area at depth E_{t1}=1 eV for each type of XLPE peelings could be estimated as in Table 1.

Hence, for any trap at depth E_t, the capture cross-section can be expressed as

$$S = (\frac{E_{t1}}{E_t})^2 S_1 \tag{13}$$

Also for the calculation of Poole-Frenkel energy lowering in Equation (2), for the sake of simplicity, the varying electric field in depolarization test is taken as an averaged equivalent value E_a. Therefore, ΔV_F for each sample type of is found in Table 2.

Combining Equations (1), (2), (7), (8), (9) and (13), it is possible to obtain values of trapping parameters E_t, N, S and intial trapped charge n_0 by knowing values of fitted parameters a, b and c and d, e and f.

2 Sample Preparation

As mentioned, cross-linked polyethylene (XLPE)

Table 1 Values of $\overline{n}_t$, E_a and S_1 for each type of samples

Type of sample	$\overline{n}_t$ /(10^{18}·m^{-3})	E_a/(MV·m^{-1})	S_1/(10^{-16}m^2)
12-year outer	6.69	2.06	1.72
12-year middle	5.52	1.70	2.29
12-year inner	9.77	3.01	9.70
8-year outer	5.56	1.71	2.25
8-year middle	5.63	1.73	2.21
8-year inner	6.79	2.09	1.67

Table 2 Values of ΔV_F for each type of samples

Type of sample	ΔV_F/eV
12-year outer	0.071
12-year middle	0.065
12-year inner	0.087
8-year outer	0.065
8-year middle	0.066
8-year inner	0.072

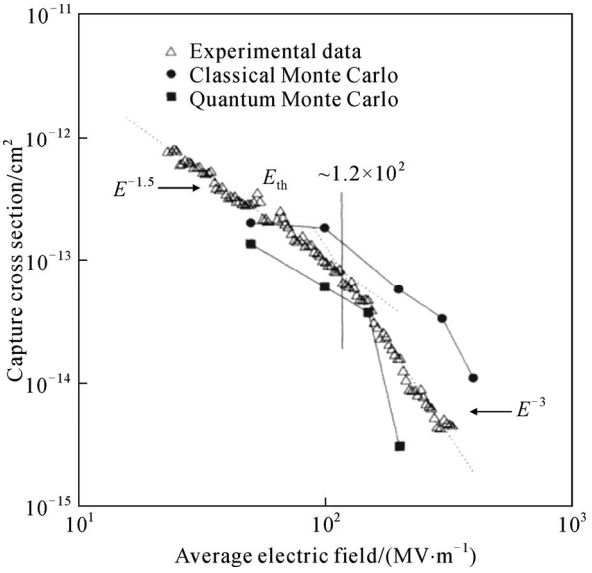

Fig.1 Capture cross-section of Coulombic attractive traps as a function of average electric field

cable sections were retired from service condition of AC 220 kV for 12 years and 8 years. The cable structure and the size are illustrated in Fig.2. The XLPE of cable insulator was sliced to films by a rotary skiver (a cutting machine to make film by rotation) from the surface of cable insulator. The thickness of obtained samples was 100~200 μm with smooth surface. For the removal of volatile chemicals in the film, the cut films were treated in vacuum oven at 80 ℃ for 48 hours for degassing[9,18].

The film samples for all the experiments were classified to several parts according to the distance from the surface of cable insulator as seen in Fig.2. In this paper, three different positions were selected as the outer (0~5 mm from surface), middle (14~18 mm), and inner (23~31 mm) layer for 12-year-operated cable and the outer (0~5 mm from surface), middle (10~15 mm), and inner (20~27 mm) layer for 8-year-operated cable

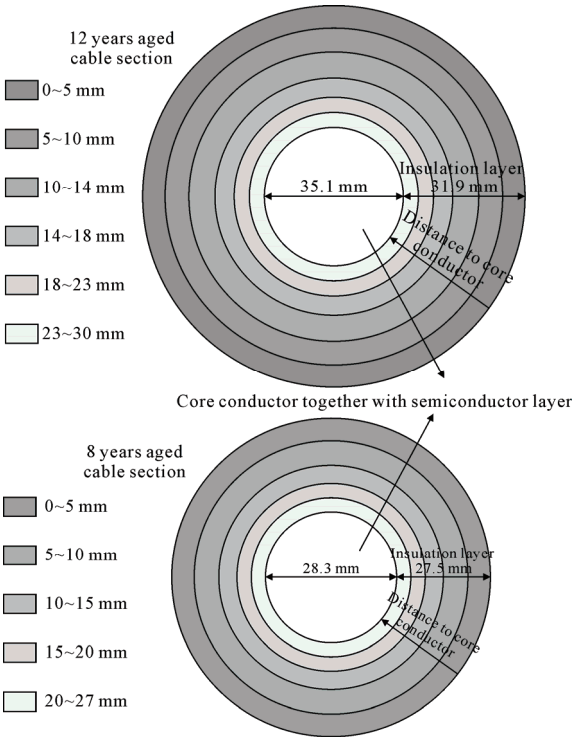

Fig.2 Cross sections and grouping method on insulation layers respectively of 12 and 8-year operated cable sections

3 Experimental

The pulsed electroacoustic (PEA) technique was used for observing dynamics of charge profiles and measurements were made for 30 minutes (described as t_e=1 800 seconds above) after the removal of the applied voltage. For XLPE films with different thickness, the applied voltage was adjusted so the applied field was fixed at 40 MV/m for all the samples. The time of the applied voltage was 6 minutes.

4 Results of Charge Dynamics

Typical results of charge decay dynamics of XLPE films from 12-year-operated and 8-year-operated cables were shown in Figs.3 to 8. Particularly for the results in Fig.6, only decay of the injected positive charge peak was observed. For Fig.3 and Fig.7, bipolar injected charges were observed but not obvious: the injected electrons gradually move to the left side and eventually become an image charge peak on the cathode. This phenomenon is more common for measurements on samples from the outer and middle layers. And for Figs.4, 5 and 8, clear bipolar injected charges decay could be observed, indicating electron

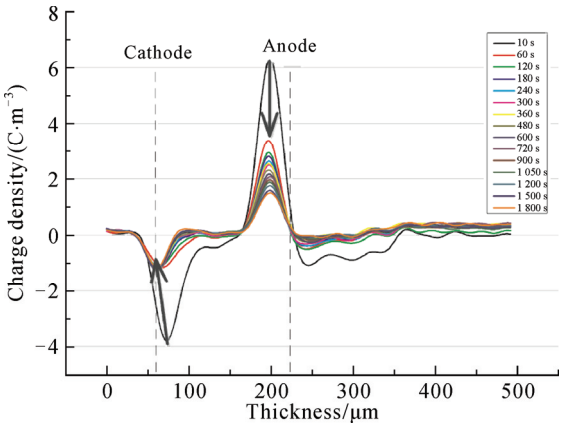

Fig.3 Charge profiles for 160 μm thick 12-year-operated XLPE at outer-layer after the removal of 6.4 kV charge

injection could be seen more clearly on inner layers. These might be caused by two reasons: 1. The resolution of the PEA measurement system is not high enough, so it was difficult to distinguish the charges of positive or negative when they are present close to each other. While two peaks of different polarities overlap with each other, only dominating charges (net charges) will be displayed on the scope 2. When samples contain more deep traps, it becomes harder for trapped electrons to escape.

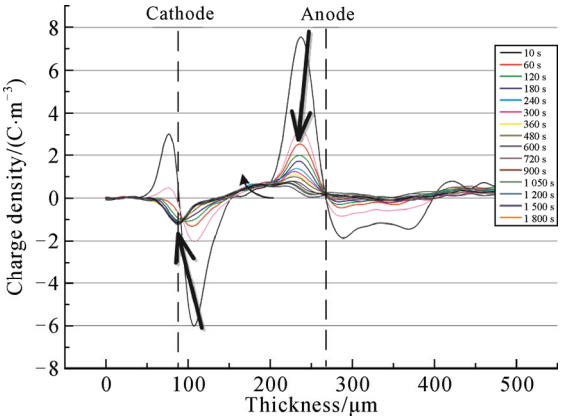

Fig.4 Charge profiles for 180 μm thick 12-year-operated XLPE at middle-layer after the removal of 7.2 kV charging voltage

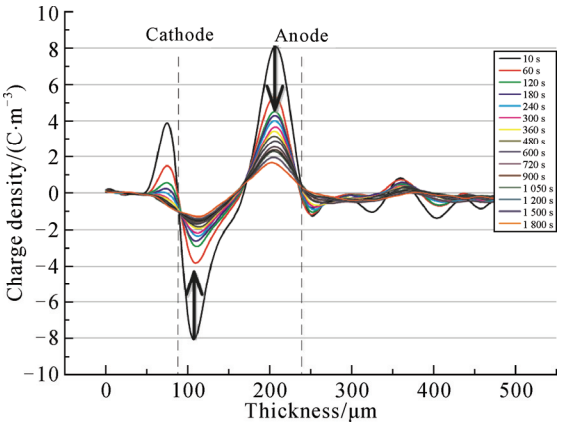

Fig.5 Charge profiles for 150 μm thick 12-year-operated XLPE at inner-layer after the removal of 6 kV charging voltage

5 Estimation of Trapping Parameters

5.1 Assumptions

The following assumptions and initial conditions were assumed for the calculation of charge trapping parameters:

1) As mentioned in previous sections, only the positive charge peak is accounted for in calculation of the charge amount.

2) Traps are uniformly distributed in the samples along film thickness.

3) Although sample slices from the same layer may have some slight differences between each other, they are assumed to be identical.

4) Since the band gap of the insulator (polyethylene) is wide, it is assumed that there are no thermally generated electrons/holesin conduction/valence band.

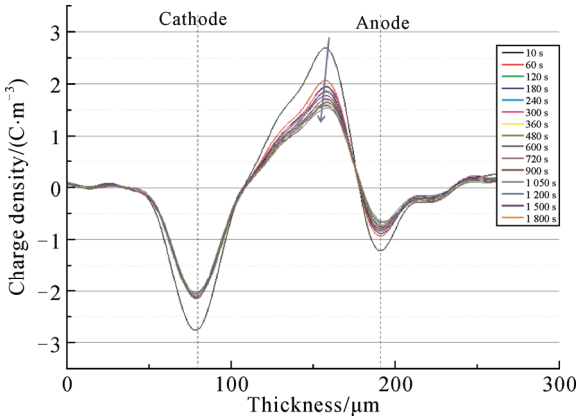

Fig.6 Charge profiles for 110 μm thick 8-year-operated XLPE at out-layer after the removal of 4.5 kV charging voltage

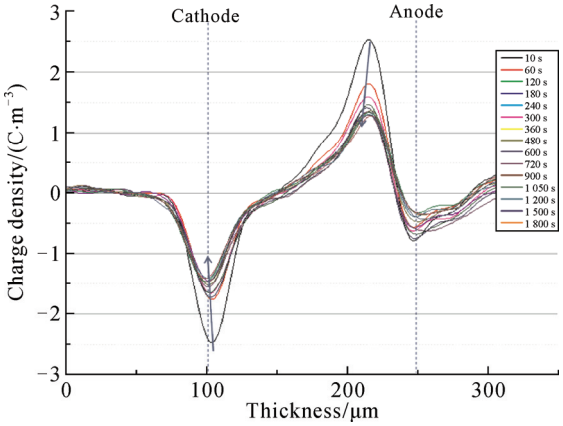

Fig.7 Charge profiles for 150 μm thick 8-year-operated XLPE at inner-layer after the removal of 6 kV charging voltage

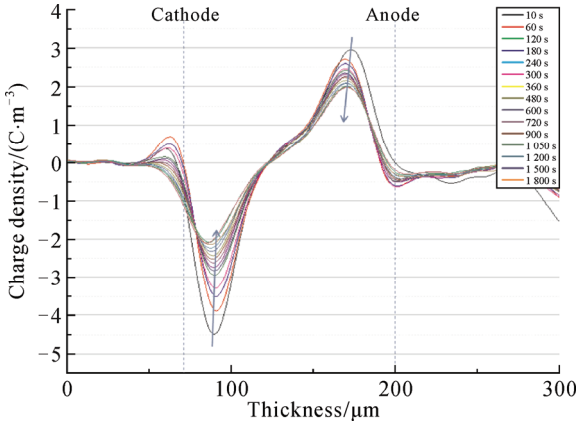

Fig.8 Charge profiles for 115 μm thick 8-year-operated XLPE at inner-layer after the removal of 4.6 kV charging voltage

5.2 Calculations

To calculate the total amount of trapped charge Q amount inside the bulk, Equation (14) has been used.

$$Q = \int_0^l |\rho(x,t)| S\mathrm{d}x \tag{14}$$

where l is the width of the positive charge layer; S is the electrode area; t is the depolarization time; and x is the distance through the film. Therefore, the number density of the trapped charges n_t is

$$n_t = \frac{Q}{lSq} \tag{15}$$

PEA measurement is rather sensitive to environmental factors such as temperature, moisture, mechanical stresses and silicone oil applied for acoustic coupling. Therefore, even though the same electric field with an identical stressing time is applied, measurement results may differ from each other. To minimize the occasional errors caused by those uncontrollable factors, measurements for each type of sample are used to calculate average number charge density. The results, with error bars, are shown in Figs. 9 and 10 for 12 year and 8 year cable samples respectively.

5.3 Curve fitting results by using charge dynamic equation

In the present paper, Equation (10), which describes a charge trapping-detrapping process after the removal of external voltage based on two energy levels, has been utilized to fit with averaged decay data, Figs.11 and 12 for 12 year and 8 year cable samples respectively. The values of fitted parameters a, b, c, d, e and f can be found in Table 3. The R-square value of each fitting result is listed in Table 4. Here R-square indicates the degree of the correlation between the experimental values and the predicted response values; values closer to 1 indicate that a greater proportion of variance is accounted for by the model.

By knowing these fitting parameters in Table 3 and also based on the calculated trapping cross section area at 1 eV for each type of samples, we could solve Equations (7), (8) and (9) and find the values of trapping parameters E_t, S and N respectively for these different samples as shown in Table 5. It should be noted that the trap depth E_t is original trap depth by adding Poole-Frenkel lowering term on the solved value, which was calculated according to Equation (2).

Table 3 Values of fitting parameters a, b, c, d, e, f

Sample type	Parameter	Outer layer	Middle layer	Inner layer
12-year cable peelings	a	-8.80×10^{17}	-9.10×10^{17}	-1.23×10^{18}
	b	-5.11×10^{-3}	-6.68×10^{-3}	-5.14×10^{-3}
	c	-5.00×10^{-2}	-5.00×10^{-2}	-5.00×10^{-2}
	d	-9.85×10^{17}	-8.00×10^{17}	-8.20×10^{17}
	e	-2.54×10^{-4}	-3.42×10^{-4}	-9.17×10^{-5}
	f	-1.06×10^{-1}	-8.67×10^{-2}	-6.46×10^{-2}
8-year cable peelings	a	-1.45×10^{18}	-1.23×10^{18}	-1.20×10^{18}
	b	-2.02×10^{-2}	-8.70×10^{-3}	-4.87×10^{-3}
	c	-2.84×10^{-1}	-3.04×10^{-1}	-3.87×10^{-1}
	d	-1.12×10^{18}	-1.33×10^{18}	-1.15×10^{18}
	e	-8.48×10^{-4}	-5.39×10^{-4}	-1.59×10^{-4}
	f	-4.31×10^{-1}	-3.99×10^{-1}	-2.59×10^{-1}

Table 4 R-square values for each type of sample by applying Equation (10)

Sample type	R-square values		
	Outer layer	Middle layer	Inner layer
12-year cable films	0.996	0.998	0.997
8-year cable films	0.997	0.996	0.985

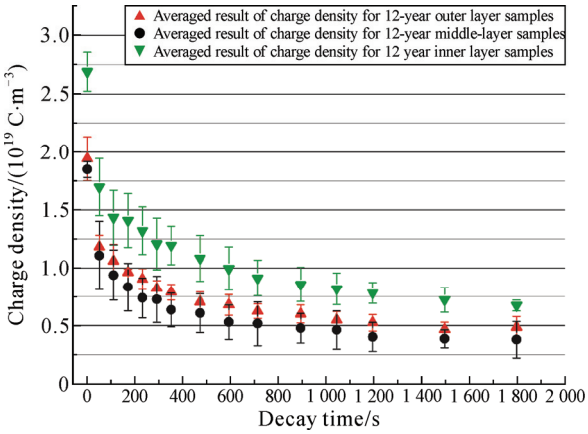

Fig.9 Averaged result for four measurements on 12-year XLPE cable films with standard deviation error bars

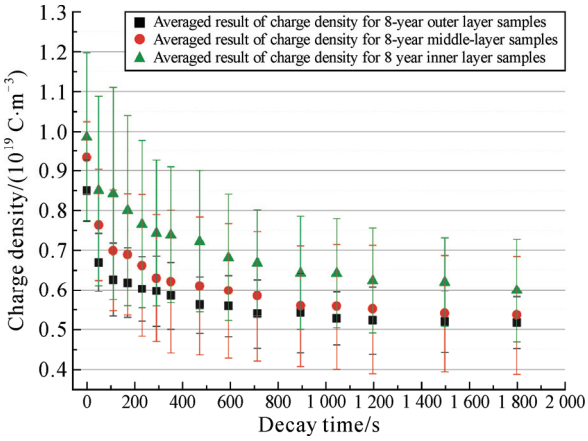

Fig.10 Averaged result for four measurements on 8-year XLPE cable films with standard deviation error bars

6 DC Breakdown Test Results

From each layer of two same cables, samples were microtomed into slices with a thinner thicknesses, (100±10) μm, for breakdown test. As was done with thicker samples for PEA test, those samples were also processed with degassing treatment in vacuum oven at 80 ℃ for 48 hours.

For these experiments, the prepared sample was tightly fixed between two sphere electrodes with diameter of 6.5 mm tightly. The external voltage was applied as ramping voltage stepping with 100 V/s from zero. Moreover, in order to avoid flashover during test, the two spherical electrodes with the tested sample in between were immersed in insulating oil. For each type of sample, 20 measurements were made to reduce statistical error.

To analyze obtained breakdown data, the Weibull distribution has been found to be a most appropriate approach to describe their stochastic behaviors[19]. Figs. 13 and 14 show the Weibull plotting of DC breakdown voltage respectively for 12-year and 8-year XLPE films respectively. The breakdown strengths for all types of sample determined by the Weibull distribution can be found in Table 6. Within 95% confidence bounds, upper and lower bounds at a characteristic value that breakdown probability equals to 63.2% (irrespective of shape factor of Weibull distribution) are also listed in Table 6.

7 Oxidation Products by FTIR Analysis

The oxidation products produced in XLPE insulator was analyzed by Fourier Transform Infra-Red (FTIR) spectroscopy. The spectrum was observed by the IR absorption in the range 400~4 000 cm^{-1} through XLPE film using a Shimadzu "IR Prestige-21" spectrometer. The spectrum was gathered by 20 scans accumulation, and the resolution was 4 cm^{-1}. In this experiment the size of samples is 10 mm×5 mm×0.1 mm. Before the experiment, samples are cleaned by alcohol and then dried. To reduce the impacts on the test results yielded by alcohol cleaning, samples must be kept for half an hour at room temperature after drying.

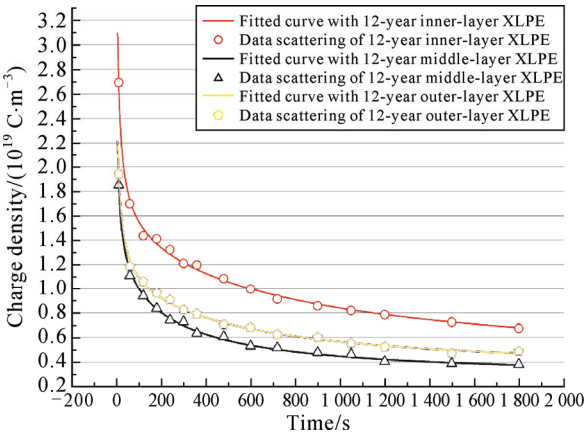

Fig.11 Curve fitting results of 12-year XLPE films from three layers using equation (10)

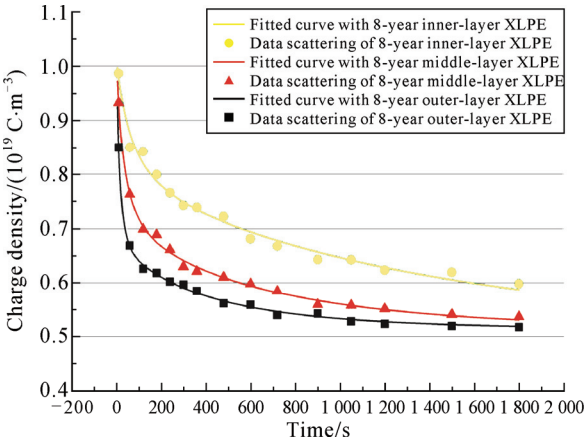

Fig.12 Curve fitting results of 8-year XLPE peelings from three layers using Equation (10)

Table 5 Trapping parameters of traps with shallow and deep energy levels by Equation (10)

Sample type	Trap type	N/m^{-3}	E_t/eV	S/m^2
Outer 12-year	Shallow traps	5.50×10^{19}	0.894	2.15×10^{-16}
	Deep traps	6.54×10^{19}	0.970	1.83×10^{-16}
Middle 12-year	Shallow traps	4.19×10^{19}	0.889	2.90×10^{-16}
	Deep traps	4.87×10^{19}	0.959	2.49×10^{-16}
Inner 12-year	Shallow traps	9.54×10^{19}	0.904	1.19×10^{-16}
	Deep traps	1.15×10^{20}	0.991	9.88×10^{-17}
Outer 8-year	Shallow traps	4.21×10^{19}	0.873	2.95×10^{-16}
	Deep traps	4.87×10^{19}	0.944	2.52×10^{-16}
Middle 8-year	Shallow traps	4.40×10^{19}	0.890	2.79×10^{-16}
	Deep traps	5.15×10^{19}	0.960	2.40×10^{-16}
Inner 8-year	Shallow traps	5.83×10^{19}	0.903	2.05×10^{-16}
	Deep traps	6.98×10^{19}	0.986	1.72×10^{-16}

Table 6 Breakdown strength for each layer of samples with 95% confidence bounds at unreliability of 63.2%

Types of XLPE films	Lower bound (95%)/(MV·m^{-1})	Breakdown strength/ (MV·m^{-1})	Upper bound (95%)/(MV·m^{-1})
12-year outer	462.80	476.70	490.63
12-year middle	472.99	487.11	500.76
12-year inner	453.07	461.28	469.08
8-year outer	476.04	493.18	509.93
8-year middle	467.78	480.32	492.46
8-year inner	455.47	468.73	481.53

Normally, absorption peaks due to carbonyl compounds should be observed between. In this range, different functional groups will have specific characteristic absorption frequency bands. Information in Table 7 is summarized from references [20-21] and values might be ±10 cm^{-1}.

From Fig.15, for 12-year cable peelings, several-peaks were found in range 1 680~1 755 cm^{-1} for 12-year cable peelings and according to Table 7, it should contain carbonyl compounds with functional groups identified as: aryl ketone (1 680~1 710 cm^{-1}, peak at 1 695 cm^{-1}), ketone (1 710~1 725 cm^{-1}, peak at 1 718 cm^{-1}), and ester (1 725~1 755 cm^{-1}, peak at 1 740 cm^{-1}). However, the peak for aryl ketone is probably caused by cross-linking byproducts acetophenone[22], hence in calculation of degree of oxidation this peak was ignored as it was not a consequence of oxidation during operation. For 8-year cable, some weak peaks observed around 1 680~1 710 cm^{-1} could be observed and were ignored for the same reason. Apart from that, a strong single carbonyl peak (range around 1 710~1 765 cm^{-1}) was found in Fig.15 for the 8-year cable and the peak value is at 1 740 cm^{-1}. It indicates that ester groups dominate among all carbonyl compounds in such samples. The absorption peak at around 2 020 cm^{-1} was least affected by the oxidation and the baseline for measuring the "invariant" peak height ranged was taken as 2 000~2 050 cm^{-1} was assumed to be the invariant peak. For the outer-layer of 8-year samples, invariant peak range become a little distorted and the valid calculation for such type of sample should be taken from 1 985~2 035 cm^{-1} Net peak height was determined by subtracting

Table 7 FTIR Absorption frequencies of functional groups containing a carbonyl (C=O)

Functional group	Wave number/cm^{-1}	Functional group	Wave number/cm^{-1}
Amide	1 650~1 700	Aldehyde	1 720~1 740
Ketone(Aryl)	1 680~1 700	Ester	1 735~1 750
Ketone(Acyclic)	1 705~1 725	Acid chloride	1 775~1 810

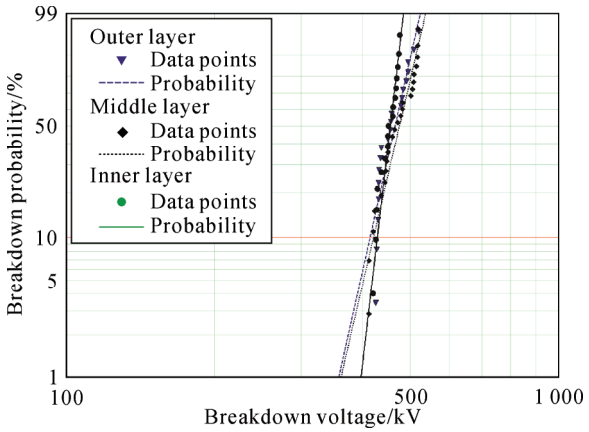

Fig.13 Weibull plot of the cumulative probability of breakdown versus breakdown voltages for 12-year operated samples

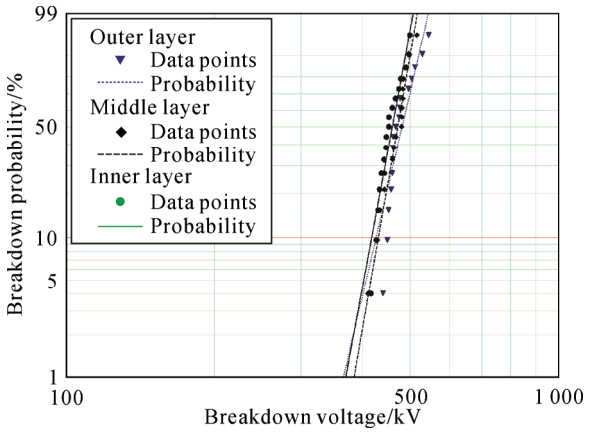

Fig.14 Weibull plot of the cumulative probability of breakdown versus breakdown voltages for 8-year operated samples

the height of the baseline immediately before the peak from the total peak height[23]. The area (intensity) of carbonyl absorption and of the invariant peak could be calculated as the area under the baseline. The carbonyl index was calculated by a ratio between oxidation peak A_{ox} and the area of invariant peak A_i[23-25], *i.e.* carbonyl index R is

$$R = \frac{A_{ox}}{A_i} \tag{16}$$

For 12-year samples, we have $A_{ox}=A_{ketone}+A_{ester}$;

whereas for 8-year samples, $A_{ox}=A_{ester}$. Therefore, the carbonyl index, that is, the yield of oxidation compounds at the depth from the surface of XLPE insulator for the two cables, was calculated based on Equation (16).

Table 8 reveals that, for both 8-year and 12-year cable sections, the relative yield of oxidation products R from outer to inner layer conforms to: $R_{out}>R_{in}>R_{min}$. This agrees to the result of 22-year cable from service condition in reference [26]. The outer-layer samples are remarkably most serious for each cable section. This should be a consequence of XLPE at the outer region having a better contact with oxygen diffusing from the external environment, hence an increase of oxidized sites.

8 Discussion

8.1 Service conditions from different insulation layers

During operation for extended periods, the samples from the inner insulation layer should experience the highest temperature and electric field [27-28]. The dependence on electric field could be found in Equation (17), which is suitable for cylindrical insulation cable of one material at AC condition[27]

$$E(r)=\frac{U}{r\ln(\frac{R_0}{R_i})} \tag{17}$$

where U stands for the applied voltage; r is the distance to the center of core conductor; R_0 is external radius of the insulation and R_i is the radius of core conductor.

Therefore, considering the diameters of core conductor illustrated in Fig.2, the electric field for 12-year cable at outer surface ($r=R_0$) equals $E(R_0)$=4.29 MV/m and for 8-year cable $E(R_0)$=4.89 MV/m, therefore we could have electric field ranges for each layer of both cable sections in Table 9. Due to scaling, the 8-year cable had operated with larger electric field than that of the 12-year cable. The electric field ranges for each layer of both cable sections are given in Table 9.

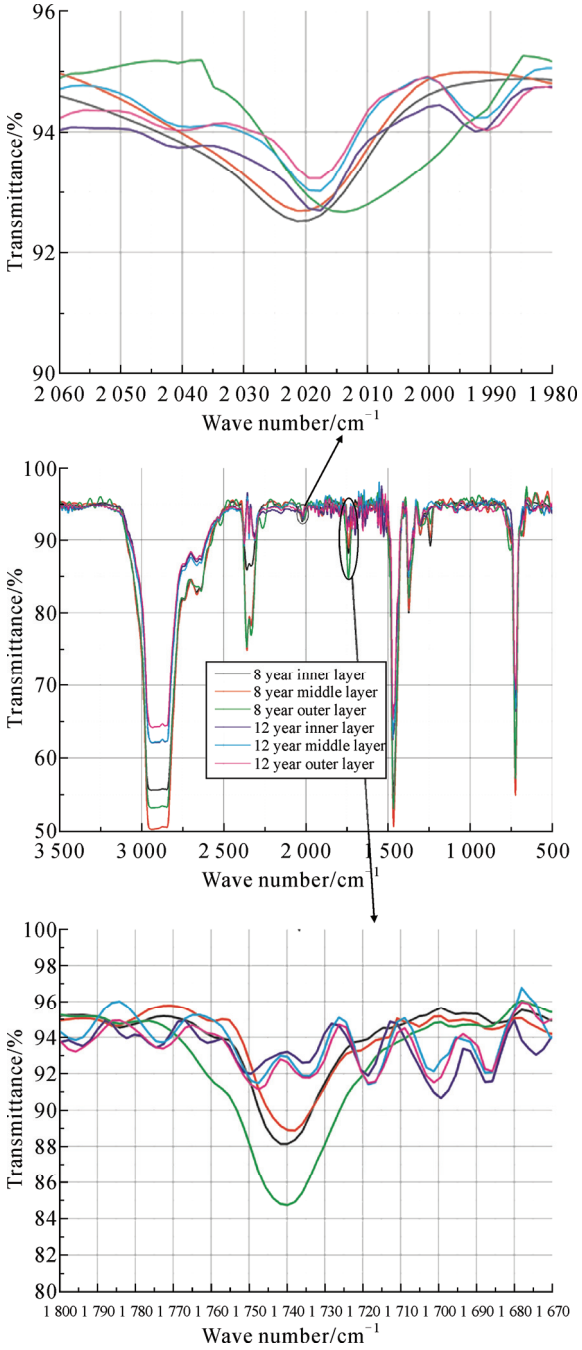

Fig.15 FTIR spectrum of 12-year and 8-year operated cable peelings from different layers with zoom-in peaks with in region 1 670~1 800 cm^{-1} and 1 980~2 060 cm^{-1}

Table 8 Relative yield of oxidation products of two types of XLPE cable peelings at three layers

Cable type	Carbonyl index		
	Outer layer	Middle layer	Inner layer
12-year cable	4.19	2.54	3.19
8-year cable	3.71	1.97	2.48

Table 9 Relative electric fields of layers of XLPE cable peelingsrespectively for two different cable sections

Cable type	Electric field/(MV·m^{-1})		
	Outer layer	Middle layer	Inner layer
12-year cable	4.29~4.76	5.96~6.74	8.02~10.90
8-year cable	4.89~5.52	6.45~7.62	9.39~13.89

8.2 Shallow and deep trapping parameters and FTIR results

The model used in the present paper treats all traps in the materials as equivalent energy levels: shallow and deep traps.

They can be correlated with physical and chemical defects. The physical defects could be recognized as changes of morphological structure, crystallinity and molecular weight whereas chemical defects refer to the oxidized sites and other new chemical constituents[10,29]. Trap density and depth are apparently greatest at the inner layer for both cables. Moreover the trapping parameters appear to be greatest for the 12-year old cable samples. The significant increase of trapping parameters at the inner layer could be attributed to the most severe service condition being experienced at this location and, as such, the highest amount of physical and chemical defects were produced in the inner region during the extended periods of operation.Comparing middle and outer layer for both cables, their trapping parameters are relatively near to each other. In more details, for 12-year cable, the trapping parameters at outer layer is a little larger than that of middle whereas for 8-year cable, both trapping parameters at outer layer, especially the trap depth, is obviously at lowest-level among all types of samples.

Looking into FTIR results, it could be found that at inner layer carbonyl index is larger than that at middle layer. This might be due to that in inner layer, amounts of oxidation products were produced under highest field and temperature, reflecting by greatest trapping parameters at inner layer for both cable sections. However, outer layer trapping parameters is lower than that at inner layer. It might be explained that more factors rather than oxidation products will contribute to deep traps, which is considered to be related with chemical changes in the materials.

8.3 Trapping parameters vs. Breakdown strengths

Plotting trap densities (shallow, deep and their sum) against breakdown strengths for each type of sample, as shown in Fig.16, it can be seen that when trap density increases breakdown strength declines. Additionally, in Fig.17, when plotting both shallow and deep trap depths versus breakdown voltages, a clear relationship between trap depth and breakdown strength indicates that when the trap depth increases, the breakdown strength decreases.

Electrical breakdown of dielectric materials is defect-related[30]. In the present paper, we quantize the defects as trapping parameters estimated from the established model. In reference [31], it was found that breakdown voltage relates to the crystal structure of polymer materials: with an increased ratio of amorphous region, the breakdown strength reduces. As mentioned earlier, the change in crystallinity could be considered as an introduction of physical defects, and therefore increasing the number of shallow traps into materials[5-7,10]. This can explain the correlation between breakdown strength and shallow trap density in Fig.16. From another angle, in DC breakdown test, greater trap density or trap depth in materials (especially deep traps) will make it will be harder for trapped charges get out of localized states. The distortion of local electric field in the bulk material will therefore become more severe and this should lead to earlier material failure. Above all, the ageing and degradation in materials might be monitored by change in trapping parameters estimated from the present model.

9 Conclusions

Through the experimental and numerical simulation works in the present paper, several conclusions can be drawn as below:

1) For both different-year aged cables, trap density and trap depth of inner layer are generally larger than that from the other two layers. This should be caused by the severest condition (highest temperature and electric field) experienced during operation duration.

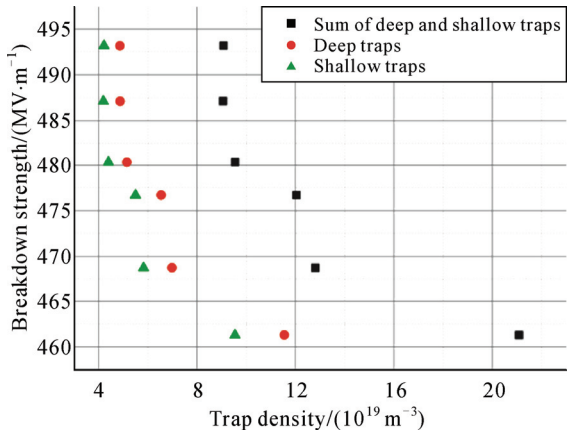

Fig.16 Plotting of trap density estimated for different samples versus breakdown strengths

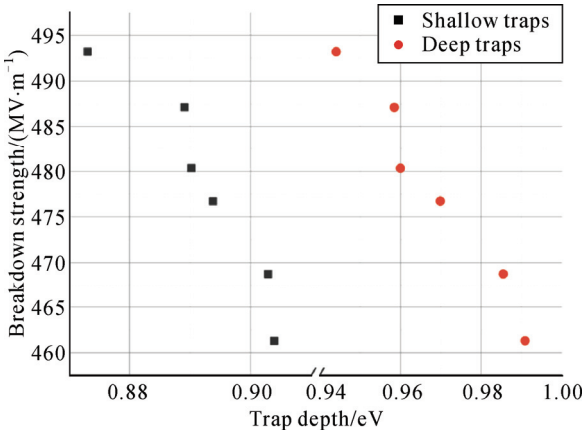

Fig.17 Plotting of trap depths estimated for different samples versus breakdown strengths

2) From FTIR measurement results, the degree of oxidation among three layers could be found by the carbonyl index values. The oxidation degree of aged cable at the outer layer is remarkably higher than that at the other two layers due to most sufficient contact with oxygen diffusing from external environment. The inner-layer samples for both cables have higher values of carbonyl index than samples from middle layer. This could be explained by more oxidation products yielded at most severe service condition in the inner layer.

3) The DC breakdown strength shows a decreasing trend with the increasing of trap density and depth. This indicates the approach proposed in the present paper might be utilized as the tool to monitor degradation and ageing in materials.

References

[1] Dissado L, Mazzanti G, Montanari G. The incorporation of space charge degradation in the life model for electrical insulating materials[J]. IEEE Transactions on Dielectrics and Electrical Insulation, 1995, 2(6): 1147-1158.

[2] Dissado L, Mazzanti G, Montanari G. A new thermo-electrical life model based on space-charge trapping[C]// IEEE International Symposium on Electrical Insulation. Montreal, Canada: IEEE, 1996: 642-645.

[3] Crine J P. A molecular model to evaluate the impact of aging on space charges in polymer dielectrics[J]. IEEE Transactions on Dielectrics and Electrical Insulation, 1997, 4(5): 487-495.

[4] Kao K C. Dielectric phenomena in solids with emphasis with physical concepts of electronic processes[M]. [s.n.]: Elsevier Academic Press, 2004: 345-347.

[5] Chen G, Xu Z. Charge trapping and detrapping in polymeric materials[J]. Journal of Applied Physics, 2009, 106(12): 123707.

[6] Zhou T, Chen G, Liao R. Charge trapping and detrapping in polymeric materials: trapping parameters[J]. Journal of Applied Physics, 2011, 110(4): 043724.

[7] Liu N, Chen G. Modeling of charge trapping/detrapping characteristics in polymer materials and its relation with ageing[C]// 2013 Annual Report, Conference on Electrical Insulation and Dielectric Phenomena. Shenzhen China: IEEE, 2013.

[8] Dissado L A, Griseri V, Peasgood W, *et al*. Decay of space charge in a glassy epoxy resin following voltage removal[J]. IEEE Transactions on Dielectrics and Electrical Insulation, 2006, 13(4): 903-916.

[9] Tzimas A, Rowland S M, Dissado L A. Effect of electrical and thermal stressing on charge traps in XLPE cable insulation[J]. IEEE Transactions on Dielectrics and Electrical Insulation, 2012, 19(6): 2145-2154.

[10] Marsacq D, Hourquebie P, Olmedo L, *et al*. Effects of physical and chemical defects of polyethylene on space charge behavior[C]// 1995 Annual Report, Conference on in Electrical Insulation and Dielectric Phenomena.Virginia Beach, USA: IEEE, 1995: 672-675.

[11] Dissado L, Fothergill J. Electrical degradation and breakdown in polymers[M]. 9th ed. London, UK: Peters Peregrinus Ltd., 1992.

[12] Canali C, Majni G, Minder R, *et al*. Electron and hole drift velocity measurements in silicon and their empirical relation to electric field and temperature[J]. IEEE Transactions on Electron Devices, 1975, 22(11): 11-13.

[13] Afanas V, Revesz A, Brown G, *et al*. Deep and shallow electron trapping in the buried oxide layer of SIMOX structures[J]. Journal of the Electrochemical Society, 1994, 141(10): 2801-2804.

[14] Blaise G, Sarjeant W. Space charge in dielectrics: energy storage and transfer dynamics from atomistic to macroscopic scale[J]. IEEE Transactions on Dielectrics and Electrical Insulation, 1998, 5(5): 779-808.

[15] Simmons J, Tam M. Theory of isothermal currents and the direct determination of trap parameters in semiconductors and insulators containing arbitrary trap distributions[J]. Physical Review B, 1973, 7(8): 3706-3713.

[16] Buchanan D, Fischetti M, Dimaria D. Coulombic and neutral trapping centers in silicon dioxide[J]. Physical Review B, 1991, 43(2): 1471-1486.

[17] Mazzanti G, Montanari G C, Alison J. A space-charge based method for the estimation of apparent mobility and trap depth as markers for insulation degradation-theoretical basis and experimental validation[J]. IEEE Transactions on Dielectrics and Electrical Insulation, 2003, 10(2):

187-197.

[18] Suh K, Hwang S, Noh J, *et al*. Effects of constituents of XLPE on the formation of spacecharge[J]. IEEE Transactions on Dielectrics and Electrical Insulation, 1994, 1(6): 1077-1083.

[19] Khalil M. The role of $BaTiO_3$ in modifying the dc breakdown strength of LDPE[J]. IEEE Transactions on Dielectrics and Electrical Insulation, 2000, 7(2): 261-268.

[20] Silverstein R M, Bassler G C, Morrill T C. Spectrometric identification of organic compounds[M]. 4th ed. New York, USA: John Wiley and Sons, 1981.

[21] Bell C, Taber D, Clark A. Chapter 11: infrared absorption spectrescopy[M]// Organic chemistry laboratory: standard and microscale experiments, 3rd ed. [s.n.]: Brooks Cole, 2001.

[22] Andrews T, Hampton R.The role of degassing in XLPE power cable manufacture[J]. IEEE Electrical Insulation Magazine, 2006, 2(6): 5-16.

[23] Stark N, Matuana L. Surface chemistry changes of weathered HDPE/wood-flourcomposites studied by XPS and FTIR spectroscopy[J]. Polymer Degradation and Stability, 2003, 86(1): 1-9.

[24] Wu Q, Qu Q, Xu Y, *et al*. Surface photo-oxidation and photostabilization of photocross-linked polyethylene[J]. Polymer Degradation and Stability, 2000, 68(1): 97-102.

[25] ASTM Standard F2102 Standard guide for evaluating the extent of oxidation in polyethylene fabricated forms intended for surgical implants[S]. West Conshohocken, USA: ASTM International, 2013.

[26] Li W, Li J, Wang X, *et al*. Physico-chemical origin of space charge dynamics for aged XLPE cable insulation[J]. IEEE Transactions on Dielectrics and Electrical Insulation, 2014, 21(2): 809-820.

[27] Jeroense M J P, Morshuis P H F. Electric fields in HVDC paper-insulated cables[J]. IEEE Transactions on Dielectrics and Electrical Insulation, 1998, 5(2): 225-236.

[28] Adel-Salam T S, Hackam R, Chikhani A Y. Temperature distribution in the dielectric insulation of distribution cables[C]// 1990 Annual Report, Conference on Electrical Insulation and Dielectric Phenomena. Pocono Manor, USA:IEEE, 1990:514-519.

[29] Meunier M, Quirke N, Aslanides A. Molecular modeling of electron traps in polymer insulators: chemical defects and impurities[J]. Journal of Chemical Physics, 2001, 115(6): 2876-2881.

[30] Shatzkes M, Av-Ron M. Statistics of defect related breakdown[C]// 19th Annual Reliability Physics Symposium. Las Vegas, USA: 1981, IEEE: 210-211.

[31] Park K, Kim J, Han S. Relation crystal structure with breakdown of polyethylene thin film[C]// 5th International Conference on Properties and Applications of Dielectric Materials. Seoul, Korea: IEEE, 1997: 662-655..

Ning Liu (S'13) was born in Anhui, China in 1990. He has received the B.Sc. degree from University of Liverpool and now he is a second-year Ph.D. candidate from EEE group of University of Southampton. His research interest mainly focus on the space charge trapping/detrapping phenomenon and modelling in polymeric materials. His paper/poster 'Investigation of charge trapping parameters in aged XLPE cables at different locations' won the first prize in Jicable 2013 HVDC conference in Perpignan, France.

George Chen (SM'11) was born in China in 1961. He received the B.Eng. (1983) and M.Sc. (1986) degrees in electrical engineering from Xi'an Jiaotong University, China. After he obtained the Ph.D. degree (1990) from the University of Strathclyde, UK, on the work of permanent changes in electrical properties of irradiated low-density polyethylene, he joined the University of Southampton as post-doctoral research fellow and became a senior research fellow subsequently. In 1997 he was appointed as a research lecturer and promoted to a Reader in 2002. He is now the professor of high voltage engineering at the University of Southampton and a visiting professor of Xi'an Jiaotong University. Over the years, he has developed a wide range of interests in high voltage engineering and electrical properties of materials and published over 300 papers.

Yang Xu (M'05) was born in Shaanxi, China in 1969.He received the B.Sc., M.Sc. and Ph.D. degrees inelectrical engineering from XJTU, Xi'an, China, in1991, 1994 and 2005, respectively. He is an associate professor of XJTU. His research interest lies inelectrical insulation measurements. He is a member of IEC TC112 (Evaluation and qualification of electrical insulating materials and systems) WG6 and also a member of the CIGRE SC B1 WG 28.

Received date 2014-11-25
Editor XIAO Zheng